Thermal conductivity and bulk viscosity in quartic oscillator chains

G. R. Lee-Dadswell,* B. G. Nickel,† and C. G. Gray‡
Department of Physics, University of Guelph, Guelph, Ontario, Canada, N1G 2W1
(Received 18 March 2005; published 19 September 2005)

We propose a relation which predicts the low-frequency thermal conductivity of a one-dimensional (1D) system from the thermal conductivity and bulk viscosity at higher frequency. Our theory is based on the assumption that "ballistic" transport by sound waves dominates the heat transport. For a system with equal heat capacities ($c_p=c_v$) this relation is particularly simple. We test the prediction by simulating a chain of particles with quartic interparticle potentials under zero pressure conditions. As the frequency $\omega\to 0$ the theory predicts that the energy current power spectrum diverges as $\omega^{-1/2}$, not seen in previous simulations. Because we simulate very long chains to long times we do observe the crossover into this regime. The bulk viscosity of a 1D chain has been determined via simulation. It is found to be finite for our system, in contrast to the thermal conductivity which is infinite.

DOI: 10.1103/PhysRevE.72.031202 PACS number(s): 44.10.+i, 05.70.Ln, 63.22.+m

I. INTRODUCTION

The criteria for a system to obey Fourier's law of heat conduction remain shrouded in mystery. While in three dimensions all systems seem to obey Fourier's law, in one dimension (1D) there is no known way to predict whether a system will obey it. Most 1D systems do not obey Fourier's law but there are some exceptions (see, for example, Refs. [1–5]). A thorough summary of past work in this area can be found in a recent review article [6].

It has been suggested by many authors [5,7,8] that, in 1D systems not obeying Fourier's law, heat is transmitted through the system by long-wavelength sound modes which pass through the system essentially undamped. This idea is backed up by the space and time-dependent heat current correlation function shown in Ref. [8], which shows energy propagation through the FPU-β system at a constant velocity. In that paper it is argued that the very well known slow diffusion of energy out of the long-wavelength modes for FPU systems may allow those modes to act as "undamped transport channels." It was also consideration of this picture of "ballistic transport" dominating heat flow which led to the design of the first 1D system which was shown to have a finite thermal conductivity [1]—the "ding-a-ling" model. It would be satisfying to put this idea of ballistic heat transport on a firmer theoretical footing and to see whether this appealing physical picture can lead directly to any predictions or explanations of how heat flow in 1D systems should behave. Few attempts have been made in this direction. For an exception to this see Ref. [8] in which this physical picture has been employed to attempt to explain the observed behavior of 1D systems (but also see comments in Ref. [9] and in our Appendix).

Though they were originally investigated as a toy model for a crystal, 1D oscillator chains are in many respects more similar to fluids. In particular, they demonstrate diffusion and a lack of long-range order [10]. In most past studies the heat transport is considered in isolation from other transport. The fluidlike nature of 1D systems suggests that it makes sense to study them via hydrodynamics, coupling the heat, momentum and mass transport modes. A calculation by Narayan and Ramaswamy using hydrodynamics has recently been published [9] in which a universal scaling law for heat transport is predicted. However, these authors recognize that this appears to be inconsistent with some simulations and must speculate on the cause(s). We believe progress in understanding is best made by simulation studies that go beyond simple power law comparisons and pay careful attention to amplitudes as well. This in turn requires that we also consider the bulk viscosity, which has been ignored in all previous simulation work on 1D systems. The bulk viscosity is the zero-frequency limit of the momentum current power spectrum. Where it is considered at all, the momentum current power spectrum is generally assumed to diverge as $\omega^{-1/2}$. This is the assumption, for example, in Ref. [9]. This is probably based on old predictions from mode-coupling theory such as Refs. [11,12]. The assumption of a divergence of the momentum current power spectrum is likely reasonable but we are unaware of previous work to verify this behavior. While we believe that this may be the most common case we show in this paper that it is not universal. Indeed, in contrast to the thermal conductivity, we will find strong evidence that the bulk viscosity of our chosen system is finite. One would expect, through mode coupling, that this different behavior of the bulk viscosity would lead to different behavior in the thermal conductivity.

Fourier's law of heat conduction is $\mathbf{J}_q=-\kappa\boldsymbol{\nabla}T(\mathbf{r},t)$ where $\mathbf{J}_q$ is the macroscopic heat flux density, $T(\mathbf{r},t)$ is the local temperature, and κ is the thermal conductivity. Newton's law of bulk viscous dissipation is $\mathbf{J}_p=-\zeta\boldsymbol{\nabla}\cdot\mathbf{v}(\mathbf{r},t)$, where $\mathbf{J}_p$ is the macroscopic momentum current density, ζ is the bulk viscosity, and $\mathbf{v}(\mathbf{r},t)$ is the local macroscopic velocity field. We ignore shear viscosity since it is irrelevant for 1D systems. The sense in which most 1D systems do not obey Fourier's law is that κ fails to converge to a finite macro-

*Electronic address: dadswell@physics.uoguelph.ca
†Electronic address; bgn@physics.uoguelph.ca
‡Electronic address: cgg@physics.uoguelph.ca

scopic value. Rather, κ is seen to go as N^{α}, where N is the number of particles in the chain and α is some power. The value of α is a matter of great interest, with different values being reported for different systems. Values typical of oscillator systems are 0.37 (reported for the FPU-β system) to 0.44 (reported for FPU-α and diatomic Toda systems) [6]. Recently $\alpha=1/3$ has been predicted [9]. Results are available in a variety of other systems such as $\alpha=2/5$ for a "quasi-1D" harmonic system with transverse modes [13], and for systems of hard point particles [6,14] where $\alpha=1/3$ has been reported.

κ and ζ are formally related to the generalized or wave-vector and frequency-dependent transport coefficients $\kappa(k,\omega)$ and $\zeta(k,\omega)$ by [15]

$$\kappa = \lim_{\omega\to 0} \hat{\kappa}(\omega) = \lim_{\omega\to 0}\lim_{k\to 0} \kappa(k,\omega), \tag{1a}$$

$$\zeta = \lim_{\omega\to 0} \hat{\zeta}(\omega) = \lim_{\omega\to 0}\lim_{k\to 0} \zeta(k,\omega). \tag{1b}$$

Here and in the following we use the notation

$$\lim_{k\to 0} A(k) \equiv \hat{A}. \tag{2}$$

The frequency-dependent $\hat{\kappa}(\omega)$ and $\hat{\zeta}(\omega)$ can be written as Green-Kubo relations in terms of the corresponding equilibrium heat current correlation function (HCCF) $\hat{C}_{\kappa}(t)$ and momentum current correlation function (MCCF) $\hat{C}_{\zeta}(t)$, namely,

$$\hat{\kappa}(\omega) = \lim_{t\to\infty} \frac{\beta^2 k_B}{2} \int_{-t}^{t} dt' e^{i\omega t'} \hat{C}_{\kappa}(t'), \tag{3a}$$

$$\hat{\zeta}(\omega) = \lim_{t\to\infty} \frac{\beta}{2} \int_{-t}^{t} dt' e^{i\omega t'} \hat{C}_{\zeta}(t'), \tag{3b}$$

where k_B is Boltzmann's constant and $\beta=1/k_BT$ is the inverse equilibrium temperature. In terms of the corresponding currents $\hat{j}_{\mu}(t)$, where $\mu=\kappa$ or ζ, we have

$$\hat{C}_{\mu}(t) \equiv \lim_{L\to\infty} \frac{1}{L} \langle \delta\hat{j}_{\mu}(t)\, \delta\hat{j}_{\mu}(0)\rangle, \tag{4}$$

where L is the system length, $\langle\cdots\rangle$ denotes a canonical average, and $\delta\hat{j}_{\mu}(t)$ is the $k\to 0$ limit of the deviation of $j_{\mu}(k,t)$ from its equilibrium value. A further remark on the definition of $\hat{j}_{\mu}(t)$ is warranted. It is, following Eq. (2), the zero k limit of the current density $j_{\mu}(k,t)$. In the case of the heat current density this is equivalent to what is often referred to as the "total heat flux," $J_{\kappa}(t)\equiv\sum_{i=1}^{N} j_{\kappa}(x_i,t)$ (x_i is the position of the ith particle) in studies where Green-Kubo relations are used to calculate thermal conductivities [6].

The HCCF $\hat{C}_{\kappa}$ in the Green-Kubo relation above can freely be exchanged with the *energy* current correlation function ECCF, $\hat{C}_{\epsilon}$ [15] defined analogously to $\hat{C}_{\kappa}$ but with the heat flux density $\hat{j}_{\kappa}$ replaced with the energy flux density $\hat{j}_{\epsilon}$ according to Eq. (5) below. Numerically, it is more convenient to calculate the ECCF and this is what we do in the simulations reported in this paper. In practice, we work with the Fourier transformed versions or power spectra of the correlation functions $\tilde{\hat{C}}_{\mu}(\omega)$. We will refer to these as the momentum current power spectrum (MCPS) and the energy current power spectrum (ECPS).

II. COUPLING OF MODES WITH BALLISTIC HEAT TRANSPORT

Consider our assumption that the transport of energy in the system is dominated in the thermodynamic limit by transport via sound waves. We write our 1D energy density and energy current density as equilibrium values $\bar{\epsilon}$ and $\bar{j}_{\epsilon}$ plus local fluctuations $\delta\epsilon(x,t)$ and $\delta j_{\epsilon}(x,t)$. Thus, our energy current correlation function is

$$\hat{C}_{\epsilon}(t) = \lim_{L\to\infty} \frac{1}{L} \langle \delta\hat{j}_{\epsilon}(t)\, \delta\hat{j}_{\epsilon}(0)\rangle. \tag{5}$$

In the usual hydrodynamic picture, every mode is coupled to every other mode. Under our assumption that sound modes should dominate energy transport, the zero k limit of the energy current fluctuation $\delta\hat{j}_{\epsilon}$ should have terms corresponding to contributions by sound modes of all wave vectors

$$\delta\hat{j}_{\epsilon}(t) = \sum_{k'} \delta\hat{j}_{\epsilon}(k',t). \tag{6}$$

For clarity, it should be stressed that $\delta\hat{j}_{\epsilon}(k',t)$ is *not* the wave vector k' mode of δj_{ϵ} [which would be denoted $\delta j_{\epsilon}(k',t)$], but rather the contribution to its $k=0$ mode due to sound modes of wave vector k' (note the hat which indicates a $k=0$ quanitity). Continuing with the usual hydrodynamic picture, the overall amplitude of the contribution to the energy current by the sound mode is $c\,\delta\epsilon(k',t)$, where c is the thermodynamic speed of sound and $\delta\epsilon(k',t)$ is the k' component of the energy density. The amplitude of particle density fluctuations due to a sound mode damps exponentially with a damping constant of $\frac{1}{2}\Gamma k'^2$ where Γ is the sound damping coefficient, which is a property of the system. But the mode amplitude of the energy density goes as the square of the mode amplitude of the particle density, so the energy density fluctuation must be

$$\delta\epsilon(k',t) = \delta\epsilon(k',0) e^{-\Gamma k'^2 |t|}. \tag{7}$$

Our use of a single sound damping coefficient, Γ, in the foregoing argument is naive. At the microscopic level we ought to expect that each sound mode has its own damping coefficient $\Gamma_{k'}$. Hence, the contribution to $\delta\hat{j}_{\epsilon}$ due to a single sound mode of wave vector k' is

$$\delta\hat{j}_{\epsilon}(k',t) = c\,\delta\epsilon(k',0) e^{-\Gamma_{k'} k'^2 |t|}. \tag{8}$$

The contribution due to this mode to the $k=0$ limit of the ECCF (5) is thus $c^2\langle[\delta\epsilon(k',0)]^2\rangle e^{-\Gamma_{k'}k'^2|t|}/L$. The amplitude in the harmonic limit is $\langle[\delta\epsilon(k',0)]^2\rangle = 1/\beta^2$. Fourier transforming and summing over modes yields the ECPS

$$\tilde{\hat{C}}_\epsilon(\omega) = \frac{2c^2}{L\beta^2}\sum_{k'} \frac{\Gamma_{k'}k'^2}{\omega^2 + (\Gamma_{k'}k'^2)^2}, \tag{9}$$

where the sum is over the whole reciprocal lattice, restricted to the number N of particles in the system; this is in the spirit of the Debye model. Together with the approximation of constant speed of sound, this means that Eq. (9) will not be valid if ω is so large that the large k' modes contribute significantly. Note that our assumption of a constant c will also only be valid for the lowest frequencies and that, more generally, the speed of sound should be brought inside the sum and replaced with a wave-vector-dependent speed of sound $c_{k'}$ calculated from a dispersion relation appropriate to the system. We will examine how significant an effect this is below.

The sound damping coefficient in 1D is formally given by $\Gamma=(\gamma-1)\kappa/(\rho c_p)+\zeta/\rho$, where $\gamma=c_p/c_v$ is the ratio of the specific heat capacities, c_p and c_v are the specific heat capacities per unit mass at fixed pressure and volume, respectively, ρ is the mass density, and ζ and κ are given by Eq. (1). But the limiting values of ζ and κ in Eq. (1) may not exist in 1D so it is not obvious how to interpret this expression for Γ. We make the simplest assumption possible—namely, that since a mode at wave vector k' oscillates at frequency $\omega'=ck'$ in the hydrodynamic limit we need only make the replacements $\Gamma \to \Gamma_{k'}$, $\kappa \to \hat{\kappa}(\omega')$ and $\zeta \to \hat{\zeta}(\omega')$. In summary, the fundamental assumption of this paper is that Eq. (9) is correct with $\Gamma_{k'}=\Gamma_{\omega'/c} \equiv \Gamma(\omega')$ and

$$\Gamma(\omega') = (\gamma-1)\hat{\kappa}(\omega')/(\rho c_p) + \hat{\zeta}(\omega')/\rho \tag{10}$$

with $\hat{\kappa}(\omega')$ and $\hat{\zeta}(\omega')$ given by Eq. (3). In particular, we assume that the wave-vector k' plays no role other than to define the frequency of the mode and hence its damping. The absence of explicit k' dependence is not *a priori* obvious nor motivated by any theory, but our simulations suggest that it is true.

Note that Eq. (9) implies that the ECPS at ω is dominated by modes k' for which $\Gamma_{k'}k'^2 \simeq \omega$. Typically the frequency of a dominant contributing mode is much greater than ω. This means that our picture of 1D systems is that of a mode "cascade" rather than mode "coupling." Each mode affects modes of much lower ω, but high ω modes are largely unaffected by low ω ones. This lack of back action makes analytical calculation very tractable. Specifically, Eq. (9) has a problem in that the ECPS depends on itself through its dependence on $\kappa_{k'}$. However, this is eased since $\tilde{\hat{C}}_\epsilon(\omega)$ is totally dominated by contributions from frequencies much higher than ω. On the other hand, the frequencies in this cascade rapidly become very small which will make confirmation by simulation challenging. For an illustration of this see the Appendix.

III. CASES OF INTEREST

The foregoing arguments make it clear that we ought to be interested in the low-frequency behavior of the MCPS (and, thus, the bulk viscosity). There has been relatively little attention paid to this in the literature. One of the few predictions of the bulk viscosity in 1D is contained in Refs. [11,12], where the leading order terms of all of the transport coefficients are calculated through mode coupling. In Ref. [11] the leading large t term of the MCCF, specialized to 1D, is given as

$$\hat{C}_\zeta(t) \simeq \left[\frac{M_{+-}}{(\Gamma)^{1/2}} + \frac{M_{HH}}{(2D_T)^{1/2}}\right]\left(\frac{1}{4\pi t}\right)^{1/2}, \tag{11}$$

where $D_T=\kappa/\rho c_p$ is the thermal diffusivity and

$$M_{+-} = \frac{1}{\beta^2}\left[1 - \frac{\gamma-1}{\alpha_p T} + \frac{\rho}{c}\left(\frac{\partial c}{\partial \rho}\right)_s\right]^2, \tag{12a}$$

$$M_{HH} = \frac{1}{2\beta^2}(\gamma-1)^2\left[1 - \frac{1}{\alpha_p c_p}\left(\frac{\partial c_p}{\partial T}\right)_p + \frac{1}{\alpha_p^2}\left(\frac{\partial \alpha_p}{\partial T}\right)_p\right], \tag{12b}$$

where $\alpha_p=-\rho^{-1}(\partial\rho/\partial T)_p$ is the thermal expansion coefficient, s is the entropy per particle and p is the pressure.

Equation (11) suggests that the low-frequency behavior of the MCPS should go as $\omega^{-1/2}$ in 1D. However, let us now restrict our attention to a 1D oscillator chain with only even powers in the interparticle potential at zero pressure. Such a system has $\gamma=1$ which implies $\alpha_p=0$ through simple thermodynamics. One term in Eq. (12b) is zero trivially due to $\gamma=1$. Terms with α_p in the denominator drop out when we realize that $\alpha_p \sim (\gamma-1)^{1/2}$ and $(\partial\alpha_p/\partial T)_p \sim (\gamma-1)^{1/2}$. Finally, a simple but tedious calculation shows that, in a 1D oscillator chain with only even powers in the interparticle potential at zero pressure, we have $(\partial c/\partial\rho)_s=-c/\rho$, and so the remaining term in Eq. (12a) cancels with the 1 inside the square brackets. Thus the $t^{-1/2}$ term of the MCCF should vanish in a 1D oscillator system with $\gamma=1$. The next order terms in 1D are probably of the form $t^{-1/2}\exp(-At)$ for some constant A (see Eq. (22) in Ref. [11]). We conclude that the integral of the MCCF should converge for a 1D oscillator system with $\gamma=1$, yielding a finite bulk viscosity. Thus, we should consider the effect that a finite bulk viscosity and $\gamma=1$ has on Eq. (9). In this case, replacing the sum in Eq. (9) with an integral, we obtain

$$\tilde{\hat{C}}_\epsilon(\omega) = \frac{c^2}{\beta^2}\sqrt{\frac{1}{2\Gamma\omega}}, \quad \Gamma = \text{const.} = \hat{\zeta}/\rho \equiv \zeta/\rho. \tag{13}$$

Thus, for this special case we expect $\tilde{\hat{C}}_\epsilon$ to vary as $\omega^{-1/2}$ at low frequency. This is precisely the conclusion of Ref. [11] who give, analogous to Eqs. (11) and (12)

$$\hat{C}_\epsilon(t) \simeq \frac{c^2}{\beta^2\sqrt{\Gamma}}\left(\frac{1}{4\pi t}\right)^{1/2}, \tag{14}$$

where we have again specialized the expression in Ref. [11] for 1D. Fourier transformation of Eq. (14) gives Eq. (13). However, note that Eq. (14) is obtained in Ref. [11] as a general result for 1D chains whereas we obtain Eq. (13) only for the special case of $\gamma=1$.

Now let us turn to the more general case of $\gamma \neq 1$. For the purposes of illustration let us interpret Eq. (11) naively and

assume that in this case $\hat{\zeta} \sim \omega^{-1/2}$ for low frequencies (but see comments in the Appendix where we put $\hat{\zeta}$ and $\hat{\kappa}$ on equal footing). If we make the further, reasonable, assumption that $\hat{\kappa}(\omega) \sim \omega^{-\alpha}$ with $\alpha < 0.5$, consistent with other theoretical predictions and numerical evidence, then Eq. (9) will be dominated by the $\hat{\zeta} \sim \omega^{-1/2}$ behavior and we will have $\Gamma(\omega') \simeq \Gamma_0 \omega'^{-1/2}$. Once again replacing the sum in Eq. (9) with an integral, we obtain

$$\tilde{\tilde{C}}_\epsilon(\omega) = \frac{4c^3}{3\beta^2(\Gamma_0 c)^{2/3}} \omega^{-1/3}, \quad \Gamma = \Gamma_0 \omega^{-1/2}. \tag{15}$$

It is worth comparing Eq. (15) to the result obtained in Ref. [9]. In that paper the authors also use $\hat{\zeta} \sim \omega^{-1/2}$, and they also obtain $\hat{\kappa} \sim \omega^{-1/3}$. We will not consider this case further here but defer it to a future paper.

In light of the above we choose, for now, to study a system with pure quartic interparticle potentials at zero pressure. This makes $\gamma = 1$ and hence

$$\Gamma_{k'} = \frac{\hat{\zeta}(\omega')}{\rho} = \frac{\beta}{2\rho} \tilde{\tilde{C}}_\zeta(\omega' = ck'). \tag{16}$$

Thus, in this preliminary test of our assumptions we will not have to worry about multiple causes, i.e., both viscous and thermal damping. The Hamiltonian is

$$H = \sum_{i=1}^{N} \left[\frac{p_i^2}{2m} + \frac{B}{4}(x_i - x_{i-1} - a)^4 \right], \tag{17}$$

where N is the number of particles in the system, p_i and x_i are the momentum and position of the ith particle, a is the equilibrium particle spacing, m is the particle mass, B is a force constant, and where we use $x_0 \equiv x_N - L$ to produce periodic boundary conditions. As is usual in studies of oscillator systems, we do not impose any further restrictions on particle positions. Of course the particle order is fixed by the fact that the force on a particle i depends only on the distances to particles $i-1$ and $i+1$ and the labeling of particles is not allowed to change.

We calculate the equilibrium thermodynamic properties of the system both to check our simulation and in order to be able to give a value for c in Eq. (9). The particle spacing a is arbitrary and, with a pure power law potential, constants such as B contribute only as scale factors. Therefore, without loss of generality, we can set $B=1$, $m=1$ and $a=1$. We carry out all simulations with $\beta=1$, $P=0$. In these units and at these conditions the thermodynamic speed of sound is $c = \left[\frac{1}{2}\Gamma(1/4)/\Gamma(3/4)\right]^{1/2} \simeq 1.216$ and the mean energy is $\langle E \rangle = 3N/4$. We go over from spatial coordinates to a particle counting scheme (Euler to Lagrange). Hence, from this point on our spatial Fourier transform is defined as

$$j_\mu(k,t) = \frac{1}{\sqrt{N}} \sum_{s=1}^{N} j_\mu^{s-1/2}(t) e^{iks}, \tag{18}$$

where $k = \{-(N-1)\pi/N, \ldots, -2\pi/N, 0, 2\pi/N, \ldots, \pi\}$ and $j_\mu^{s-1/2}$ is the current between particles s and $s-1$. The momentum and energy currents are

TABLE I. Comparison of the analytically predicted thermodynamic sums with values from simulations. Errors on numerical results are simply the standard error of the results from the simulations.

Quantity	Analytical prediction	Numerical result
$\langle E \rangle / N$	3/4	0.749 ± 0.007
$\langle \delta \hat{j}_\zeta^2 \rangle$	0.549	0.547 ± 0.008
$\langle \delta \hat{j}_\epsilon^2 \rangle$	1.014	1.008 ± 0.06

$$j_\zeta^{s-1/2} = \tau_{s-1/2} \equiv -(x_s - x_{s-1} - 1)^3, \tag{19a}$$

$$j_\epsilon^{s-1/2} = (\dot{x}_s + \dot{x}_{s-1})\tau_{s-1/2}/2, \tag{19b}$$

where $\tau_{s-1/2}$ is just the local stress. The $k=0$ current fluctuations $\langle [\delta \hat{j}_\mu(t)]^2 \rangle$ are useful for checking thermodynamic sum rules. We find

$$\langle [\delta \hat{j}_\zeta(t)]^2 \rangle = \frac{6\Gamma(3/4)}{\Gamma(1/4)} - \frac{1}{2}\frac{\Gamma(1/4)}{\Gamma(3/4)} \simeq 0.549, \tag{20a}$$

$$\langle [\delta \hat{j}_\epsilon(t)]^2 \rangle = \frac{3\Gamma(3/4)}{\Gamma(1/4)} \simeq 1.014. \tag{20b}$$

IV. NUMERICAL RESULTS

We have used molecular dynamics simulations of our system. We integrate with an eighth order symplectic algorithm because symplectic integrators produce no secular terms in the system energy [16,17]. We constructed our algorithm from precision improved versions of the coefficients presented as "solution D" in Table 2 of Ref. [16]. For each run, the system to be integrated is initialized to an equilibrium state by using ensemble statistics. We then change coordinates to a frame with zero total momentum. This step is important to prevent advective contributions in our $\tilde{\tilde{C}}_\mu$ [9]. Many runs were averaged to produce approximate canonical ensemble averages of calculated quantities. We tracked the errors in energy, momentum and center of mass position as a check. Integration was carried out on the Shared Hierarchical Academic Research Computing Network (SHARCNET), which is a network of HP/Compaq processors in parallel. Typical runs on 8 processors with 2^{14} particles for 2^{22} time units and a time step of 0.125 time units ran for $2 \times 10^5 s$ ($\sim$2 days).

The sums over all particles of the momentum current $\hat{j}_\zeta(t)$ and energy current $\hat{j}_\epsilon(t)$ were output so that we could calculate the $k=0$ modes of the ECCF and MCCF. Additionally, $\langle E \rangle$, $\langle \delta \hat{j}_\zeta^2 \rangle$ and $\langle \delta \hat{j}_\epsilon^2 \rangle$. The averages of these thermodynamic sums were averaged over all runs of the simulations and are within a standard error of the expected values (Table I).

Calculating $\tilde{\tilde{C}}_\mu(\omega)$ directly is impractical. We instead calculate $\langle |\tilde{\hat{j}}_\mu(\omega)|^2 \rangle$ and note that

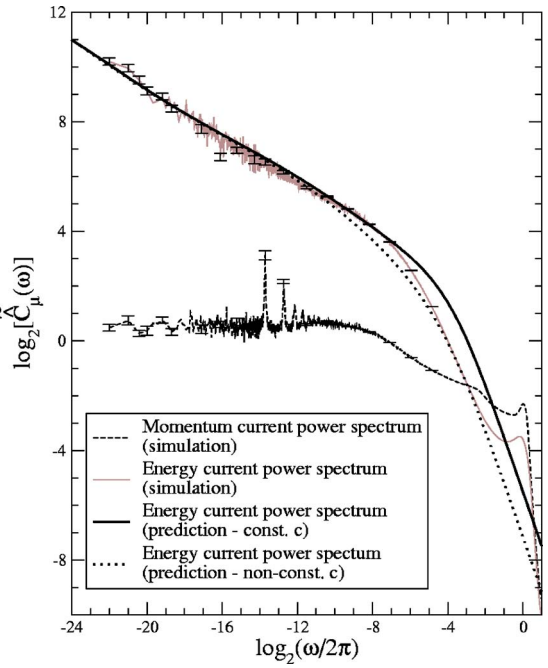

FIG. 1. (Color online) The ECPS and MCPS for a quartic oscillator chain. The predicted ECPS was calculated using Eq. (9). Error bars on selected points represent one standard deviation errors.

$$\langle|\tilde{\delta}\tilde{j}_\mu(\omega)|^2\rangle = t\int_{-t}^{t} dt'\left(1-\frac{|t'|}{t}\right)e^{i\omega t'}\hat{C}_\mu(t') \simeq t\tilde{\hat{C}}_\mu(\omega), \tag{21}$$

where t is a large time (ideally $t\to\infty$). At the lowest frequency examined, $2\pi/t$, this approximation causes an error of only 3%. The error drops off quickly over the region of interest (by $2000\pi/t$ the error is 0.007%). Having thus computed $\tilde{\hat{C}}_\epsilon(\omega)$ and $\tilde{\hat{C}}_\zeta(\omega)$ for each run, we averaged over all runs. The results for 49 runs at $N=2^{14}$, $t=2^{22}$ are shown in Fig. 1 and, on expanded scales, Figs. 2 and 3. Data at higher ω has been "binned" for clarity. Binning reduces the noise

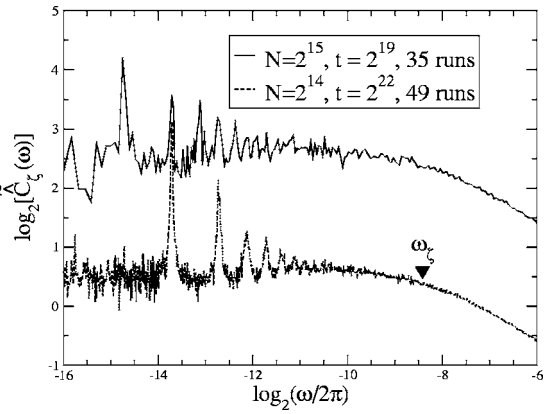

FIG. 2. Low-frequency part of $\tilde{\hat{C}}_\zeta(\omega)$ for two system sizes. The top curve has been shifted up by 2 units. The "corner" frequency ω_ζ is obtained from the fit to the MCPS (see text).

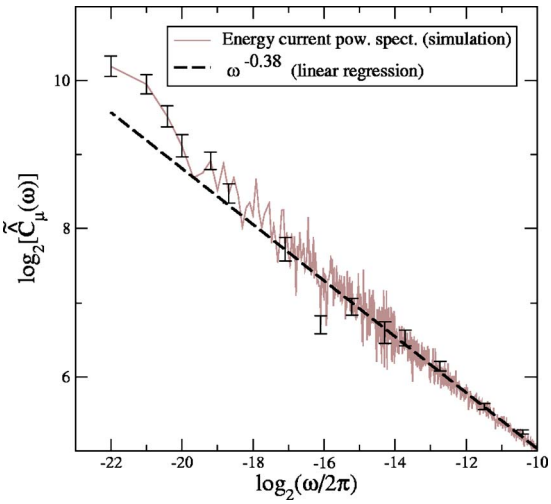

FIG. 3. (Color online) Low-frequency part of $\tilde{\hat{C}}_\epsilon(\omega)$ with trend line showing $\omega^{-0.38}$ behavior at intermediate frequencies and deviation from that behavior at lower frequencies. The linear regression line is calculated on the range from $\omega/2\pi=2^{-16}$ to $\omega/2\pi=2^{-10}$ and extrapolated to lower frequencies.

level without washing out significant structure. The ECPS is similar to the one reported for the FPU-β system in Ref. [8]. The series of peaks in the MCPS are at the lowest sound mode frequencies $\omega_i/2\pi=ck_i/2\pi=(c/Na)i$ for $i=\{1,2,\ldots\}$.

We have used Eq. (9) to calculate the theoretical $\tilde{\hat{C}}_\epsilon$ using Eq. (16) to get $\Gamma_{k'}$ from the simulated $\tilde{\hat{C}}_\zeta$ (we use a fit to $\tilde{\hat{C}}_\zeta$ to generate the lowest ω parts of the theoretical ECPS partly to reduce "noise" and partly for numerical convenience). A comparison of our theoretical prediction for the ECPS with the simulation results can be seen in Fig. 1. The predicted $\tilde{\hat{C}}_\epsilon$ follows the simulated one very closely at all but the highest frequencies. It should be stressed that the theoretical curves in Fig. 1 have no adjustable parameters. The inputs to the theoretical curve are only the simulated MCPS and the hydrodynamic speed of sound, c and these determine all properties of the curve including its overall amplitude. The discrepancy at high ω can be explained by the breakdown of the hydrodynamic approximation. The magnitude of this breakdown is estimated by comparison with the predicted curve in which the dispersion relation $\omega'=2c\sin(k'/2)$ is used to give a reasonable nonconstant c. The simulation data at most frequencies (but see Fig. 4) lies between the curves generated with the two dispersion relations. The frequency integrals of the two theoretical curves differs by a factor of 2. This is mostly because of the high-frequency behavior which dominates the integral. The two theoretical curves become virtually indistinguisable at very low frequencies, as we would expect.

The low ω peaks in the MCPS raise a question about its $\omega\to 0$ behavior; is it approaching a constant value or are there progressively higher peaks as $\omega\to 0$? We can address this question by looking at Fig. 2 which shows the low ω parts of the MCPS for two system sizes. The figure clearly shows that the peaks are simply pushed to lower frequencies, leaving a zero slope region at frequencies above the peaks.

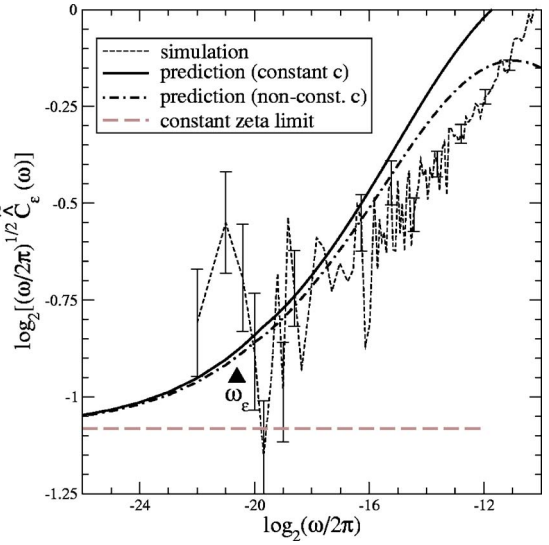

FIG. 4. (Color online) The ECPS multiplied by $\omega^{1/2}$. The horizontal grey line is the ζ=constant prediction (13). The "corner" frequency ω_ϵ is explained in the text. The "constant c" theoretical curve was calculated using $\omega'=ck'$ whereas the "nonconstant c" curve was calculated using $\omega'=2c\sin(k'/2)$. Note that Figs. 1 and 3 show that the ECPS is essentially featureless (i.e., it has no peaks) in the frequency range from $\omega/2\pi=2^{-19}$ to 2^{-10}. Because of this, we have carried out additional binning of the simulation data in that region for this plot in order to make the overall trend of the data more obvious.

Presumably, in the limit of an infinite system the peaks would be pushed to zero frequency leaving the entire power spectrum for frequencies above $\omega/2\pi\simeq 2^{-10}$ with zero slope. This, combined with the prediction from Eq. (11) is strong evidence that the MCPS is converging to a finite value (implying a finite bulk viscosity ζ). The MCPS is fit between $\omega=6\times10^{-4}$ and 1×10^{-1} by the empirical relation

$$\tilde{\hat{C}}_\zeta=\frac{A}{[1+(\omega/\omega_\zeta)^2]^{1/4}}, \tag{22}$$

where $A=1.56$, $\omega_\zeta=1.83\times10^{-2}$, where $\chi^2=480$ on a fit over 425 points. This indicates a bulk viscosity for the system of $\zeta=A/2=0.78$.

The power law behavior of the ECPS changes at very low frequency due to the onset of a regime in which the sum in Eq. (9) is dominated by the flat portion of the MCPS. Figure 3 shows a linear regression to the ECPS between $\omega/2\pi=2^{-16}$ and $\omega/2\pi=2^{-10}$ (the clearly linear region). For these intermediate frequencies, the ECPS goes as approximately $\omega^{-0.38}$. However, the extrapolation to lower frequencies shows that there is a clear divergence from $\omega^{-0.38}$ at very low frequencies where the ECPS seems to go as a higher power of ω (see further remarks in the next paragraph where we discuss the apparent approach to $\tilde{\hat{C}}_\epsilon\sim\omega^{-1/2}$). No single power law is able to fit the whole region below $\omega\simeq1.5\times10^{-3}$. Indeed, the lowest frequency points deviate from the linear regression by over 4 standard deviations. Even if they are included in the linear regression all of the lowest frequency points deviate from the fit line by over three standard deviations.

The nature of the changing behavior is made much more obvious in Fig. 4 in which we see that $\omega^{1/2}\tilde{\hat{C}}_\epsilon$ appears to be going asymptotically to the prediction in Eq. (13). The frequency ω_ϵ of the "corner" in $\tilde{\hat{C}}_\epsilon$ can be determined from the amplitude and "corner" frequency ω_ζ of $\tilde{\hat{C}}_\zeta$. The high-frequency limit of Eq. (22) is $\Gamma(\omega\gg\omega_\zeta)\simeq A(\omega_\zeta/\omega)^{1/2}/2$. So we may use Eq. (15) with $\Gamma_0=A\omega_\zeta^{-1/2}/2$ to obtain

$$\tilde{\hat{C}}_\epsilon(\omega\gg\omega_\epsilon)=\frac{1}{3}\left[\frac{2^8c^7}{A^2\omega_\zeta}\right]^{1/3}\omega^{-1/3}. \tag{23}$$

The intercept of Eq. (23) with Eq. (13) yields a "corner" frequency for the ECPS of

$$\omega_\epsilon=\frac{3^6}{2^{16}}\frac{A\omega_\zeta^2}{c^2}\simeq3.93\times10^{-6}. \tag{24}$$

It is worth noting again that our theory yields $\tilde{\hat{C}}_\epsilon\sim\omega^{-1/3}$ for the $\omega>\omega_\epsilon$ region when we assume that $\tilde{\hat{C}}_\zeta\sim\omega^{-1/2}$ for $\omega>\omega_\zeta$. This is similar to the $\omega\to0$ behavior predicted in Ref. [9]. However, this is not the $\omega\to0$ behavior of this system (though we expect it to be the $\omega\to0$ behavior of many other systems). Finally, Fig. 4 shows that the theoretical prediction differs from the simulation data by a few percent around $\omega/2\pi=2^{-14}$. Because predictions based on different dispersion curves differ by the same order, this probably marks the limit of validity of the hydrodynamic approximation on which our modeling is based.

V. CONCLUSIONS

At frequencies typical of previous studies ($\omega>\omega_\epsilon$) we obtain $\tilde{\hat{C}}_\kappa\sim\omega^{-0.38}$. This is in close agreement with $\tilde{\hat{C}}_\kappa\sim\omega^{-0.37}$ reported for the FPU-β model [8]. However, at the lower frequencies studied here ($\omega\sim\omega_\epsilon$) we see strong evidence that the power law dependence is approaching $\omega^{-1/2}$ as predicted.

Our analysis suggests the following cases.

(1) In the case of a 1D oscillator system with $c_p=c_v$ we expect that the bulk viscosity is finite (consistent with the mode coupling predictions in Ref. [11]) and the low-frequency limiting behavior of the ECPS should be $\tilde{\hat{C}}_\epsilon\sim\omega^{-1/2}$. This is what we see for our pure quartic system. We expect that runs to sufficiently low frequency on the FPU-β system at zero pressure should display this behavior as well.

(2) For the more general case of 1D oscillator systems with $c_p\neq c_v$ we might naively expect, also from Ref. [11], that $\hat{\zeta}\sim\omega^{-1/2}$ (which is the usual assumption) and our theory predicts $\tilde{\hat{C}}_\epsilon\sim\omega^{-1/3}$ in agreement with Ref. [9]. We are currently studying a system with cubic and quartic terms in the interparticle potential (for which $c_p\neq c_v$). Preliminary results are consistent with an infinite bulk viscosity and $\tilde{\hat{C}}_\epsilon(\omega)\sim\omega^{-1/3}$. These results will be reported in detail in a future

paper. We believe that studies of the FPU-α system will also see this behavior if pushed to low enough ω. However, there is another interpretation of these results (see the Appendix and point 3 below).

(3) The case described in point 2 above in which $\hat{\zeta} \sim \omega^{-1/2}$ may never occur. Instead the situation for $c_p \neq c_v$ may be considerably more complicated as described in the Appendix.

(4) In the case of a 1D system with a zero hydrodynamic speed of sound such as the coupled rotor system our theory predicts that the thermal conductivity should be finite (as seen in Ref. [3]). Equation (9) predicts no contribution to the ECPS due to ballistic transport if $c=0$.

(5) It is unclear whether some modified version of this theory could apply to "quasi-1D" systems with transverse modes such as that in Ref. [13].

Our key assumption has been that the heat transport in the system is dominated by "ballistic" transport via sound waves. Further, we have assumed that the Γ in the mode coupling formula for $\tilde{\hat{C}}_\kappa$ should be the $\Gamma(\omega')$ at the ω' of the contributing mode. Hence, we are able to generate a predicted curve for the ECPS which is in very good agreement with the simulated ECPS. We have used a system in which $c_p=c_v$ to simplify matters because there is no κ term in the sound damping coefficient.

This work suggests that the old idea of ballistic transport of heat in 1D oscillator systems is a *quantitatively* correct physical picture. It shows that it is possible, using this picture, to predict the low-frequency power law behavior of the ECPS and that this behavior depends critically on the low frequency power law behavior of the MCPS. Further, it shows that, because of the "mode cascade," the onset of the low-frequency limiting behavior of $\hat{\kappa}$, occurs at frequencies far lower than the onset of the limiting behavior of $\hat{\zeta}$. We suggest that much of the confusion around different values of α for different oscillator systems stems from the fact that the simulations, thus far, have not probed low enough frequencies to see the limiting behavior. We hope that this work will also spark interest in the bulk viscosity of 1D systems, which has been neglected in previous work.

APPENDIX: A TOY MODEL OF COMPLETE COUPLING OF MOMENTUM AND ENERGY TRANSPORT

Let us consider the case of a 1D chain with $\gamma \neq 1$ in more detail. In this case we expect both $\tilde{\hat{C}}_\zeta$ and $\tilde{\hat{C}}_\epsilon$ to diverge as $\omega \to 0$. This implies a divergence in both $\hat{\zeta}(\omega)$ and $\hat{\kappa}(\omega)$ and, by extension, divergences in $\Gamma(\omega')$ and $D_T(\omega')$. Thus, the denominators in the terms inside the brackets in Eq. (11) are not constants but depend on frequency and are divergent. Thus, we have reason to doubt the simple picture of $\hat{\zeta} \sim \omega^{-1/2}$, since it is not self-consistent.

The divergences in $\hat{\zeta}(\omega)$ and $\hat{\kappa}(\omega)$ will feed back into Eq. (9) via Eq. (10) as already examined. However, they will also feed back into an equation for $\tilde{\hat{C}}_\zeta(\omega)$ analogous to Eq. (9). To illustrate the essential features of this picture we investigate the toy equation

$$G(x) = \frac{2\lambda}{\pi} \int_0^\infty dy \frac{G(y) y^2}{x^2 + [G(y) y^2]^2}, \tag{A1}$$

which combines the self-consistency equation for $\tilde{\hat{C}}_\zeta$ and $\tilde{\hat{C}}_\epsilon$ into a single equation. In Eq. (A1) x is a dimensionless frequency ratio ω/ω_0 with ω_0 some characteristic frequency and $G(x)=\Gamma(x)\omega_0/c^2$ is a dimensionless damping coefficient. The sum over modes k' in Eq. (9) has been converted to the integral over dimensionless frequency y in Eq. (A1). Complicated but qualitatively unimportant thermodynamic functions that enter into the equations for $\tilde{\hat{C}}_\zeta$ and $\tilde{\hat{C}}_\epsilon$ are represented by the single dimensionless parameter λ.

The essence of Eq. (A1) is that for any small x the integral is dominated by $y \gg x$. This is completely analogous to the behavior of Eq. (9). As already described in the text after Eq. (10), this is better described as a mode cascade rather than as mode coupling. In practice this means that Eq. (A1) can be solved iteratively and, as an excellent approximation, this iteration need only be carried out once. The results of this iteration are as follows. Set

$$G_p(y) = A_p y^{-p} \tag{A2}$$

in the integrand in Eq. (A1) and assume that this is valid for all y. Then it follows that $G(x)$ on the left-hand side is

$$G_q(x) = A_q x^{-q}, \tag{A3}$$

where

$$q = \frac{1-p}{2-p}, \tag{A4a}$$

$$A_q = \frac{\lambda A_p^{1/(p-2)}}{(2-p)\cos\left(\frac{\pi}{4-2p}\right)}. \tag{A4b}$$

Of course it is to be understood that Eqs. (A2)–(A4) are only valid over restricted intervals for y and x. The boundary between two regions of the solution given by Eqs. (A2) and (A3) is found by setting $x=y=x_{pq}$ and equating $G_q(x_{pq})$ to $G_p(x_{pq})$. $G_p(y)$ is approximately valid for $y > x_{pq}$ and $G_q(x)$ for $x < x_{pq}$. The integration is to be repeated with G_q replacing G_p in the integrand. The final solution G is a concatenation of the G_p and is piecewise smooth.

Since our model only describes hydrodynamic processes, the high-frequency initialization must be obtained by other means such as numerical simulation. For our toy for illustration purposes we simply choose our starting G_p as $G_0=1$ (i.e., $p=0$). The subsequent exponents follow a Fibonacci sequence; they are $0/1, 1/2, 1/3, 2/5, \ldots$, converging on $p^* = (3-\sqrt{5})/2 \simeq 0.382$. The corresponding fixed point A^* is found by setting $A_p=A_q=A^*$ with $p=p^*$ in Eq. (A4). We denote $G^*(x)=A^* x^{-p^*}$. The result for $G(x)/G^*(x)$ for the choice of $\lambda=1$ is shown on a logarithmic scale in Fig. 5 and represents our single iteration approximation. Note that the $G_p(x)$ that make up $G(x)$ are only approximately valid over the range between the boundaries x_{pq}. This approximation is best near the midpoint between two adjacent x_{pq}. Improvement

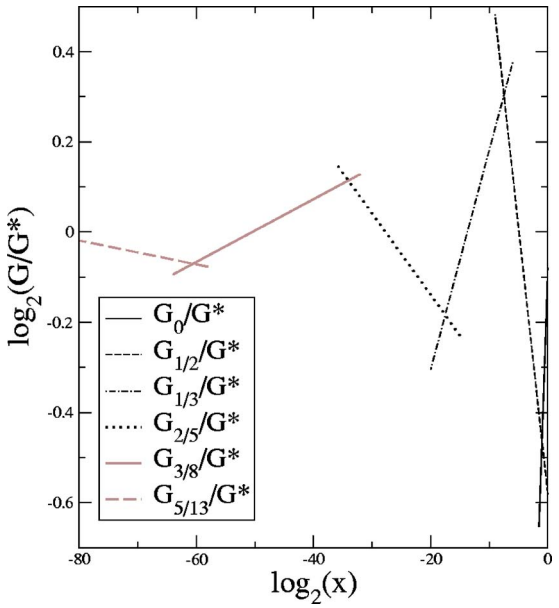

FIG. 5. (Color online) $G(x)/G^*(x)$ for $\lambda=1$, $G_0=1$ showing G_p for $p=0,1/2,1/3,2/5,3/8,5/13$.

could be obtained by carrying out another iteration using the entire piecewise smooth $G(x)$ from Fig. 5 as the integrand in Eq. (A1) and generating a new $G(x)$. This iteration process can be repeated. No qualitative change results from this other than a rounding of the function in the vicinity of the boundaries x_{pq}.

How might this toy model relate to a real hydrodynamic system? We have already seen that Eq. (A1) is analogous to Eq. (9). Equation (11) suggests that there should be an analogous equation for $\tilde{\tilde{C}}_{\zeta}$. So both the thermal conductivity and bulk viscosity might diverge at low frequency in a manner similar to our toy model. The picture here is one of an infinite regression of renormalizations. Parts of the sequence of exponents obtained here $(0/1,1/2,1/3,2/5,\ldots)$ have already been seen in other papers. For example, the work in Refs. [11,12] may be seen as a "one-step" renormalization from constant transport coefficients yielding frequency-dependent transport coefficients which go as $\omega^{-1/2}$. The more recent work in Ref. [9] can be seen as a "second step." Narayan and Ramaswamy argue in the text after their equation (5) that the momentum current correlation functions can be taken as $t^{-d/2}$ (in 1D this gives a bulk viscosity $\hat{\zeta}\simeq\omega^{-1/2}$) and from this obtain a thermal conductivity $\hat{\kappa}\simeq\omega^{-1/3}$. In Ref. [8] the authors propose a phenomenological relaxation rate for the oscillatory modes of a system γ_k—analogous to $\Gamma_k k^2$. They then, after their equation (15) propose that this relaxation rate should go as $k^{5/3}$. This is the same as $\Gamma_k\simeq k^{-1/3}$. This yields, in their analysis, a thermal conductivity $\hat{\kappa}\simeq\omega^{-2/5}$. We propose that a fundamental issue is whether there is an endpoint to the renormalizations that must be carried out in obtaining the low-frequency behavior of the transport coefficients.

If the infinite regression of renormalizations above were the correct picture then we should expect a "universal" behavior at very low frequency of ω^{-p^*} for both the thermal conductivity and the bulk viscosity. However, this universal behavior would not be reached until frequencies so low as to be, possibly, inaccessible by simulation. However, at accessible time scales both $\hat{\zeta}$ and $\hat{\kappa}$ would be seen to pass through regimes of ω^{-q} with various values of q. The exact exponents seen for any system would depend on the specific details of the high-frequency nonhydrodynamic interactions, and the lowest frequency probed by the simulations. Thus, at accessible low frequencies, the behavior of 1D hydrodynamic systems would be best described by Eq. (9) and an analogous equation for the MCPS, rather than by any specific power law divergence of the transport coefficients. If this picture is correct then attention should focus on verification of Eqs. (9) and (10) and a corresponding equation for the MCPS rather than on *cataloging* low frequency behaviors of more and more systems.

[1] G. Casati, J. Ford, F. Vivaldi, and W. M. Visscher, Phys. Rev. Lett. **52**, 1861 (1984).
[2] D. J. R. Mimnagh and L. E. Ballentine, Phys. Rev. E **56**, 5332 (1997).
[3] C. Giardiná, R. Livi, A. Politi, and M. Vassalli, Phys. Rev. Lett. **84**, 2144 (2000).
[4] T. Prosen and M. Robnik, J. Phys. A **25**, 3449 (1992).
[5] B. Hu, B. Li, and H. Zhao, Phys. Rev. E **57**, 2992 (1998).
[6] S. Lepri, R. Livi, and A. Politi, Phys. Rep. **377**, 1 (2003).
[7] J. Ford, Phys. Rep. **213**, 271 (1992).
[8] S. Lepri, R. Livi, and A. Politi, Europhys. Lett. **43**, 271 (1998).
[9] O. Narayan and S. Ramaswamy, Phys. Rev. Lett. **89**, 200601 (2002).
[10] T. Yoshida, K. Shobu, and H. Mori, Prog. Theor. Phys. **66**, 759 (1981).
[11] M. H. Ernst, E. H. Hauge, and J. M. J. van Leeuwen, J. Stat. Phys. **15**, 7 (1976).
[12] M. H. Ernst, E. H. Hauge, and J. M. J. van Leeuwen, J. Stat. Phys. **15**, 23 (1976).
[13] J. Wang and B. Li, Phys. Rev. Lett. **92**, 074302 (2004).
[14] P. Grassberger, W. Nadler, and L. Yang, Phys. Rev. Lett. **89**, 180601 (2002).
[15] D. Forster, *Hydrodynamic Fluctuations, Broken Symmetry, and Correlation Functions* (W.A. Benjamin Inc., Reading, MA, 1975).
[16] H. Yoshida, Phys. Lett. A **150**, 262 (1990).
[17] E. Forest and R. D. Ruth, Physica D **43**, 105 (1990).